



LAWRENCE
LIVERMORE
NATIONAL
LABORATORY

HOT ELECTRON ENERGY DISTRIBUTIONS FROM ULTRA-INTENSE LASER SOLID INTERACTIONS

H. Chen, S. C. Wilks, W. Kruer, P. Patel, R.
Shepherd

October 9, 2008

Physics of Plasmas

Disclaimer

This document was prepared as an account of work sponsored by an agency of the United States government. Neither the United States government nor Lawrence Livermore National Security, LLC, nor any of their employees makes any warranty, expressed or implied, or assumes any legal liability or responsibility for the accuracy, completeness, or usefulness of any information, apparatus, product, or process disclosed, or represents that its use would not infringe privately owned rights. Reference herein to any specific commercial product, process, or service by trade name, trademark, manufacturer, or otherwise does not necessarily constitute or imply its endorsement, recommendation, or favoring by the United States government or Lawrence Livermore National Security, LLC. The views and opinions of authors expressed herein do not necessarily state or reflect those of the United States government or Lawrence Livermore National Security, LLC, and shall not be used for advertising or product endorsement purposes.

HOT ELECTRON ENERGY DISTRIBUTIONS FROM ULTRA-INTENSE LASER SOLID INTERACTIONS

Hui Chen, S. C. Wilks, W. L. Kruer, P. K. Patel, R. Shepherd

Lawrence Livermore National Laboratory, Livermore, CA 94550, USA

Abstract: Measurements of electron energy distributions from ultra-intense ($>10^{19}$ W/cm²) laser-solid interactions using an electron spectrometer are presented. These measurements were performed on the Vulcan petawatt laser at Rutherford Appleton Laboratory and the Callisto laser at Lawrence Livermore National Laboratory. The effective hot electron temperatures (T_{hot}) have been measured for laser intensities ($I\lambda^2$) from 10^{18} W/cm²μm² to 10^{21} W/cm²μm² for the first time, and T_{hot} is found to increase as $(I\lambda^2)^{0.34\pm0.4}$. This scaling agrees well with the empirical scaling published by Beg et al. (1997), and is explained by a simple physical model that gives good agreement with experimental results and particle-in-cell simulations.

It is well established that high-intensity lasers incident on solid targets can generate relativistic electrons [1-4]. Knowing how the laser energy couples to the electrons in the target, and what the resulting electron energy distribution is inside the target, is of paramount importance in the understanding of virtually all short-pulse high energy density physics experiments [5-8]. In particular, as a major effort to generate controlled thermonuclear fusion, the fast ignition concept [9] relies on effective heating of solid fuel target of these short pulse laser produced hot electrons beyond the region of direct laser interaction.

Measuring the hot electron generation and transport are, however, among the most difficult experiments, since the electron distribution inside the target cannot be measured directly. Instead there are many techniques that employ indirect methods to infer the electron temperature inside the target [1, 3], such as K-alpha emission [10] and fast ions measurements [11]. These techniques have their own limitations and uncertainties, in addition to assumptions or model dependencies that are required to infer the electron distribution inside the target. Measuring the escaping electrons from the target is another approach that has been widely used [12-15]. While this measurement is clearly related to the original electron distribution in the target, it is complicated somewhat by the fact that simple models predict that during the interaction, the target will charge up to a few to several MeV, thus altering the electron energies before entering the spectrometer [16, 17].

A useful metric to quantify the hot electrons is by using the slope of the hot electron energy distribution, hereafter referred to as the effective electron temperature, T_{hot} . Assuming the slope of measurable electrons is similar to that which extends to lower energies inside the target, one can infer the T_{hot} of the electrons generated from the laser

target interaction. For laser intensities up to $I\lambda^2 = 5 \times 10^{18} \text{ Wcm}^{-2}\mu\text{m}^2$, it was found that higher laser intensity results in higher effective electron temperatures [3], and based on experimental data, Beg et al. [18] found an empirically scaling to be the effective T_{hot} scaled as $(I\lambda^2)^{0.3}$, which is referred as Beg scaling hereafter. Since then, although the laser intensity has reached far beyond $I\lambda^2 = 1 \times 10^{19} \text{ Wcm}^{-2}\mu\text{m}^2$ to $1 \times 10^{21} \text{ Wcm}^{-2}\mu\text{m}^2$, little experimental data is available on the T_{hot} scaling verse laser intensity. This paper presents measurements on two distinct lasers where we found that for ultrahigh intensities up to $I\lambda^2 = 8 \times 10^{20} \text{ Wcm}^{-2}\mu\text{m}^2$, the effective temperature scales like $(I\lambda^2)^{0.34 \pm 0.4}$, in substantial agreement with the Beg scaling derived from measurements at lower intensities. A simple physical model is shown to agree well with both experiment and particle simulations. In particular, the model also predicts a slight dependence of effective temperature on incidence angle of the laser to the target normal.

The experiments were conducted using a magnetic spectrometer [19] at the Rutherford Appleton Laboratory (RAL) Vulcan Petawatt laser facility [20] and the Callisto (previously referred as JanUSP) Ti:sapphire laser [21] at the Jupiter laser facility at Lawrence Livermore National Laboratory. RAL Vulcan Nd:glass laser delivers about 400 J of energy onto targets in a 400 fs at full-width at half-maximum (FWHM) temporal pulse onto a focal spot of about 7-8 μm at FWHM [22], containing about 60% of laser energy. The laser focal spot was measured at low energy (attenuated low energy pulses from the OPCPA) using a magnification of 40 microscope objective and 16-bit vacuum CCD directly imaging the focus of the parabola. The lineout of the focal spot profile is shown in Fig. 1. The p -polarized laser was incident with an angle of 28° to the target normal. The laser intensity reaches up to $5 \times 10^{20} \text{ W/cm}^2$. The electron spectrometer was aligned 15 degrees from the laser beam, i.e. 43 degrees off normal, and 79 cm away from the target. The parameters of the Callisto laser include a pulse length of 100 fs and delivers up to 10 J laser energy at 800 nm. The laser is focused with an f/2 parabola to a focus spot size of about 3.5 μm , and the laser intensity ranges from 10^{17} - 10^{20} Wcm^{-2} . The laser is incident on the various targets at 22.5 degrees off normal. The spectrometer was aligned 30 degrees from the laser beam, i.e. 52.5 degrees off normal, and 23 cm away from the target.

For the same target configuration (Ag target, 50 μm in thickness), the hot electron distribution varied significantly as a function of laser intensities, as illustrated in Fig. 2. For the same intensity, the electron distribution does not vary much for targets made of elements from Al to Ag, a factor of 6 different in nuclear charge Z . The T_{hot} inferred from the electron energy distribution from these experiments are plotted in Fig. 3 along with the ponderomotive scaling and Beg scaling [18]. The ponderomotive scaling [23] proposes an approximately $(I\lambda^2)^{0.5}$ dependence of T_{hot} to laser intensity:

$$kT_{\text{hot}} \sim m_e c^2 \left[\sqrt{1 + \frac{I\lambda^2}{2.8 \times 10^{18}}} - 1 \right]$$

This scaling was proposed to be valid when the plasma interaction density was close to critical density. When laser intensities become strong enough to increase the interaction

densities to well above critical, this scaling would appear to be an over-estimate, and must be modified accordingly as discussed in [23,24].

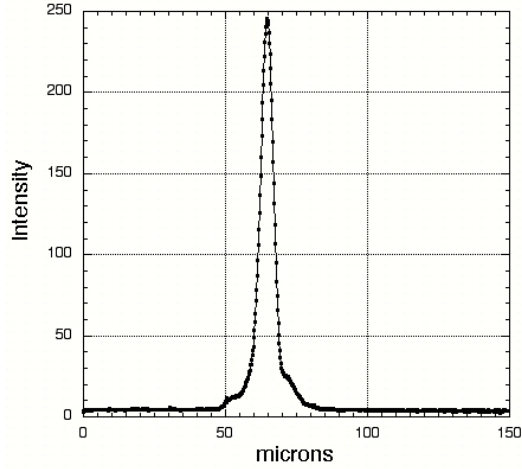


Figure1. The focal spot measured for RAL Vulcan laser.

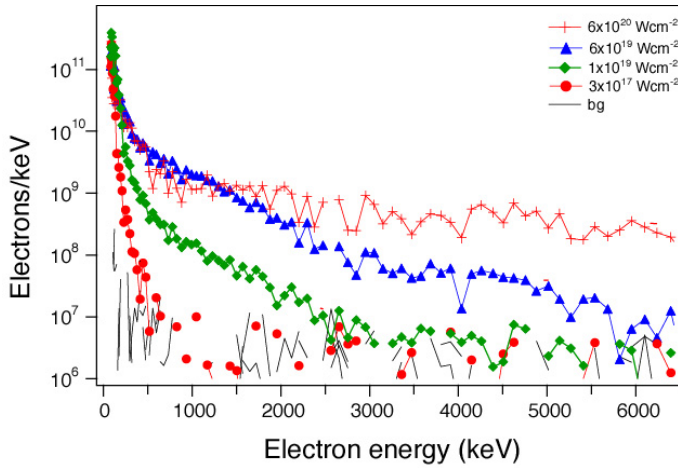


Figure 2. Electron distributions for 50 mm Ag targets at four laser intensities. The hot electron temperatures are 0.04 MeV, 0.5 MeV, 0.8 MeV and 2.8 MeV, respectively, for the four intensities from low to high order. The black line is indicative of the background levels.

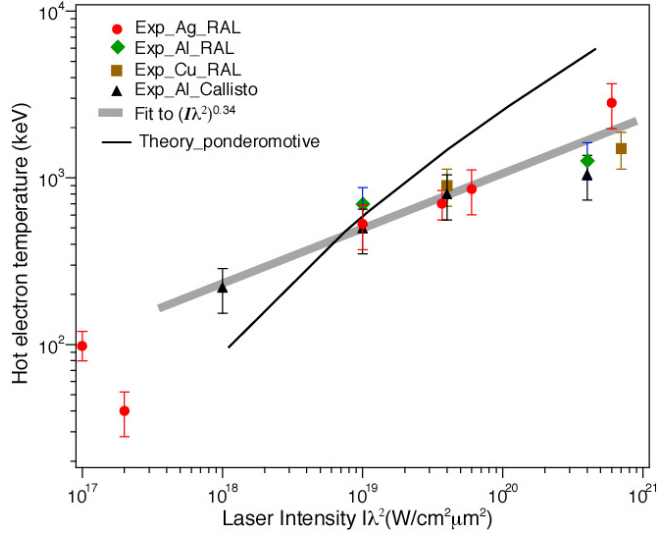


Figure 3. Experimental data of T_{hot} versus laser intensity compared with the ponderomotive-based scaling (black line) and $I^{0.34}$ scaling (which overlaps with Beg scaling ($I^{0.33}$)). Note that the experimental angle of incidence was 22 degrees to normal for Callisto, and 28 degrees for RAL.

The experimental data is simulated using a 2D particle-in-cell (PIC) code WAVE [25]. In addition, a simple physical model is presented that helps to understand this scaling. The results are shown in Fig. 4 for 1 μm laser wavelength, where the simulation and model results are plotted relative to the experimental scaling. The details of this model are as follows.

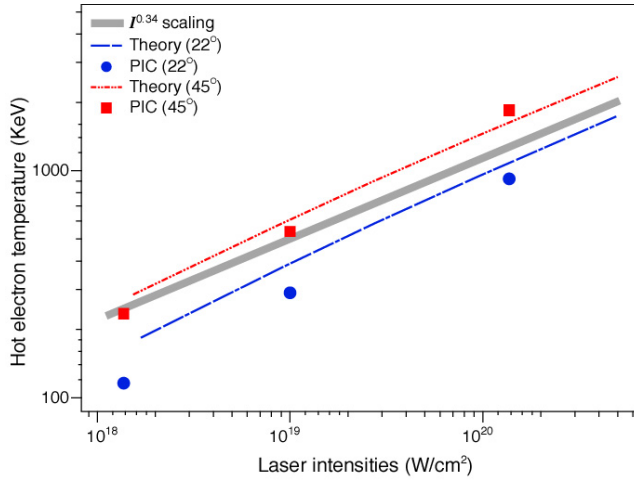


Figure 4. Simulations using the 2D PIC code WAVE (boxes, $\theta = 45^\circ$, circles, $\theta = 22^\circ$) showing temperature scaling consistent with theory presented in the text. The $I^{0.34}$ scaling is shown for comparison.

Initially, before the main pulse arrives, a prepulse will create a small amount of preplasma. For very high laser intensities, the electron density at the interaction surface near the critical surface (where the plasma frequency equals the laser frequency) quickly increases considerably due to self-steepening as the laser pressure far exceeds the material pressure at the critical surface [26]. As the density at this interface increases, the electrons that are generated there are less energetic because the shorter the skin depth of the plasma due to the increase in electron density allows for less penetration of the laser's electron-magnetic field. This results in lower hot electron temperatures since there was less electron acceleration. We can quantify this argument by requiring the electron temperature $T_{\text{eff}} = (\gamma - 1)m_e c^2$ to be equal to the driving electric field of the laser (the normal laser component, given by $E_{\text{Laser}} \sin \theta$, where θ is the angle of incidence of the laser k vector to target normal) times the distance that it acts over a relativistic skin depth, given by $c/(\gamma^{1/2}\omega_0)$. Here, γ is the usual relativistic factor for the electrons travelling near the speed of light (c), m_e the usual electron mass, and ω_0 the frequency of the laser. This results in the following equation

$$\gamma^{\frac{1}{2}}(\gamma - 1) = \sin \theta \sqrt{\frac{I\lambda^2}{1.37 \times 10^{18}}}$$

which is then solved for γ , and placed back into T_{eff} to get an effective temperature for the hot electrons. The results of doing this for 22.5 and 28 degrees (used in the two experiments) are plotted in Fig. 3 along with the experimental data. This describes the experimental data better than pure ponderomotive scaling, and is very close to that inferred from the data presented in the Beg et al., [18] publication. Clearly, this only holds when the incident angle is substantial. As one approaches normal incidence and lower intensity, a ponderomotive [23, 24] and Brunel-type heating [27] will again be better predictors of the effective temperature. An interesting outcome of this model is a clear prediction that larger angles of incidence will give higher temperatures. Usually, the error in experimentally determining the temperature is greater than the difference in temperature predicted for the two angles used in the experiments. However, we can demonstrate the effect with the 2D PIC simulations. We simulated two very different cases: 22 degrees, and 45 degrees. The simulations were carried out using the electromagnetic, relativistically correct WAVE code. The results are shown in Fig. 4. The simulations used a fixed ion plasma with a density of 40 times critical, and a scale length of $L = n_{\text{crit}} dx/dn = 0.02 c/\omega_0$. The laser, which was on for 30 fs, was quickly ramped up to a constant intensity, so that an unambiguous intensity could be used in order to compare with the theoretical prediction. The results, along with the predictions from Eq. (3), are shown in Fig. 4. For a given intensity, the simulations show a dependence of temperature on angle that is in good agreement with the theoretical predictions, as well as agreeing with the experimental data for the case of 22 degrees.

In summary, we have presented experimental measurement of hot electrons at laser intensity up to $5 \times 10^{20} \text{ W/cm}^2$. A fit to the experimental data at high intensity revealed that the scaling of hot electron temperature proportional to 0.34 power of the laser intensity.

We present a simple theory that reproduces this scaling. A side effect of this model is that it predicts a dependence of the hot electron temperature with angle. This effect was clearly observed in 2D PIC simulations.

This work was performed under the auspices of the U.S. Department of Energy by the Lawrence Livermore National Laboratory under Contract DE-AC52-07NA27344 and LDRD 08-LW-058. We thank the staff of the Central Laser Facility, CCLRC Rutherford Appleton Laboratory and the Jupiter Laser Facility for their excellent support for the experiments. We also wish to thank Drs. Max Tabak and Andreas Kemp for useful discussions, and Drs. Don Correll and William Goldstein for their support and encouragement.

References

- [1] R. A. Snavely, et. al., Phys. Rev. Lett. **85**, 2945 (2000)
- [2] M. H. Key, et al., Phys. Plasmas **5**, 1966 (1998);
- [3] P. Gibbon, "Short Pulse Interactions with Matter: an introduction", Imperial College Press (2005)
- [4] P. R. Drake, "High-energy-density physics: fundamentals, inertial fusion, and experimental astrophysics", Springer, (2005)
- [5] P. A. Norreys, et. al., Phys. Plasmas **11**, 2746 (2004).
- [6] M. H. Key, et. al., Phys. Plasmas **15**, 022701 (2008)
- [7] K. Flippo, et. al., Phys. Plasmas **15**, 056709 (2008)
- [8] H. S. Park, et. al., Phys. Plasmas **15**, 072705 (2008)
- [9] M. Tabak, et al., Phys. Plasmas **1**, 1626 (1994)
- [10] H. Chen, et al., Phys. Rev. Lett. **70**, 3431 (1993).
- [11] S. J. Gitomer, et al., Phys. Fluids, **29**, 2679 (1986).
- [12] G. Malka and J. L. Miquel, Phys. Rev. Lett. **77**, 75 (1996)
- [13] C. Gahn et al. Rev. Sci. Instrum **71** 1642 (2000)
- [14] D. F. Cai, et al., Phys. Plasmas **10**, 3265 (2003)
- [15] Y. T. Li, et al., Phys. Rev. Lett. **96**, 165003 (2006)
- [16] E. E. Fill, et al, Phys. Plasmas, **12**, 052704 (2005.)
- [17] T. Yabuuchi, et al., Physics of Plasmas, **14**, 040706 (2007)
- [18] F. N. Beg, et al, Phys. Plasmas, **4**, 447, (1997)
- [19] H. Chen, et al., Rev. Sci. Instrum. **74**, 1551, (2003).
- [20] C. N. Danson *et al.*, Nucl. Fusion **44**, S239 (2004).
- [21] J. D. Bonlie *et al.*, Appl. Phys. B **70**, S155 (2000).
- [22] P. K. Patel, et al. Plasma Phys. Control. Fusion **47** B833 (2005)
- [23] S. C. Wilks, et al., Phys. Rev. Lett. **69**, 1383 (1992).
- [24] S. C. Wilks and W. L. Kruer, IEEE J. of Quantum Electronics, **11**, 1954 (1997).
- [25] R. L. Morse and C. W. Nielson, Phys. Fluids **14**, 830 (1971).
- [26] A. J. Kemp, et. al., Phys. Rev. Lett. **101**, 075004 (2008)
- [27] F. Brunel, Phy. Rev. Lett. **59**, 52 (1987).